Cellular prion protein regulates β-secretase cleavage of the Alzheimer's amyloid precursor protein

Edward T. Parkin*†‡, Nicole T. Watt*†, Ishrut Hussain§, Elizabeth A. Eckman¶, Christopher B. Eckman¶, Jean C. Manson‖, Herbert N. Baybutt‖, Anthony J. Turner*, and Nigel M. Hooper*†**

*Proteolysis Research Group, Institute of Molecular and Cellular Biology, Faculty of Biological Sciences, and †Leeds Institute of Genetics, Health and Therapeutics, University of Leeds, Leeds LS2 9JT, United Kingdom; §Neurodegeneration Research, Neurology and Gastrointestinal Centre of Excellence for Drug Discovery, GlaxoSmithKline Research and Development Limited, Third Avenue, Harlow, Essex CM19 5AW, United Kingdom; ¶Mayo Clinic, Jacksonville, FL 32224; and ‖Roslin Institute, Neuropathogenesis Unit, Edinburgh EH9 3JF, United Kingdom

Edited by Stanley B. Prusiner, University of California, San Francisco, CA, and approved May 10, 2007 (received for review October 30, 2006)

Proteolytic processing of the amyloid precursor protein (APP) by β-secretase, β-site APP cleaving enzyme (BACE1), is the initial step in the production of the amyloid β (Aβ) peptide, which is involved in the pathogenesis of Alzheimer's disease. The normal cellular function of the prion protein (PrP^C), the causative agent of the transmissible spongiform encephalopathies such as Creutzfeldt–Jakob disease in humans, remains enigmatic. Because both APP and PrP^C are subject to proteolytic processing by the same zinc metalloproteases, we tested the involvement of PrP^C in the proteolytic processing of APP. Cellular overexpression of PrP^C inhibited the β-secretase cleavage of APP and reduced Aβ formation. Conversely, depletion of PrP^C in mouse N2a cells by siRNA led to an increase in Aβ peptides secreted into the medium. In the brains of PrP knockout mice and in the brains from two strains of scrapie-infected mice, Aβ levels were significantly increased. Two mutants of PrP, PG14 and A116V, that are associated with familial human prion diseases failed to inhibit the β-secretase cleavage of APP. Using constructs of PrP, we show that this regulatory effect of PrP^C on the β-secretase cleavage of APP required the localization of PrP^C to cholesterol-rich lipid rafts and was mediated by the N-terminal polybasic region of PrP^C via interaction with glycosaminoglycans. In conclusion, this is a mechanism by which the cellular production of the neurotoxic Aβ is regulated by PrP^C and may have implications for both Alzheimer's and prion diseases.

lipid raft | proteolysis | scrapie | glycosaminoglycan

Alzheimer's disease (AD) is characterized by the presence of extracellular senile plaques and intracellular neurofibrillary tangles within the afflicted brain. The major constituents of senile plaques are the amyloid β (Aβ) peptides, which are derived from the proteolytic processing of the amyloid precursor protein (APP) (1). In the amyloidogenic pathway, β-secretase cleavage of APP yields a soluble N-terminal fragment sAPPβ, along with a short membrane-bound C-terminal fragment that is subsequently cleaved by γ-secretase to release the Aβ peptides. In the alternative, nonamyloidogenic pathway, α-secretase cleaves APP within the Aβ sequence, thus precluding the formation of Aβ, and releases a soluble N-terminal fragment sAPPα. The transmembrane aspartyl protease, β-site APP cleaving enzyme (BACE1), has been identified as β-secretase (2), members of the ADAM (a disintegrin and metalloprotease) family, particularly ADAM10 and ADAM17, are responsible for α-secretase cleavage (3), while a complex of at least four proteins, the presenilins, nicastrin, Aph-1, and Pen-2, constitutes the γ-secretase (2).

The prion protein (PrP) is the causative agent of the transmissible spongiform encephalopathies (TSEs) that include Creutzfeldt–Jakob disease (CJD), Gerstmann-Scheinker-Straussler (GSS) disease, kuru and fatal familial insomnia in humans, bovine spongiform encephalopathy in cattle, and scrapie in sheep (4). In these diseases, the normal cellular form of PrP (PrP^C) undergoes a conformational change to the infectious form, PrP^{Sc}. The function of PrP^C remains enigmatic, with roles in metal homeostasis, neuroprotective signaling, and cellular response to oxidative stress having been proposed (5, 6).

AD and CJD share a variety of neuropathological features (7–9), and the Val/Met-129 polymorphism in the gene encoding PrP^C has been identified as a risk factor for early onset AD (10, 11). In addition, like APP, PrP^C is shed from the cell surface by zinc metalloproteases and is subject to endoproteolysis by ADAM10 and ADAM17 (12–15). As a result of these pathological, genetic, and mechanistic similarities, we were led to investigate whether PrP^C alters the proteolytic processing of APP. We show that PrP^C inhibits the β-secretase cleavage of APP and reduces Aβ formation. This effect is lost in scrapie-infected mouse brain or in cells expressing mutants of PrP associated with human prion disease. The regulation of β-secretase requires PrP^C to be located in lipid rafts and is mediated by the N-terminal polybasic region of PrP^C interacting with BACE1 via glycosaminoglycans (GAGs).

Results and Discussion

PrP^C Inhibits the β-Secretase Cleavage of APP. To investigate whether PrP^C alters the proteolytic processing of APP, the cDNA encoding murine PrP was stably transfected into SH-SY5Y cells expressing APP_{695}. In the transfected cells, PrP^C appeared as a broad band of 32 to 40 kDa due to the differentially glycosylated forms (Fig. 1*A*). The presence of PrP^C had no effect on the amount of APP_{695} holoprotein in the cell lysates (Fig. 1*B*) or on the amount of sAPPα in the cell medium (Fig. 1*C*). However, PrP^C dramatically inhibited (97.5%) the shedding of sAPPβ (Fig. 1 *D* and *E*) and reduced the secretion into the conditioned medium of $Aβ_{1–40}$ by 92% and of $Aβ_{1–42}$ to an undetectable level (Fig. 1*F*). Similarly, expression of PrP^C inhibited the amyloidogenic processing of endogenous APP in cells stably expressing BACE1 [supporting information (SI) Fig. 6]. In these cells, PrP^C reduced the amount of sAPPβ by 95% and reduced $Aβ_{1–40}$ and $Aβ_{1–42}$ to undetectable levels.

Because PrP^C decreased the production of both sAPPβ and Aβ, it can be concluded that the observed inhibitory effect is at the level

Author contributions: E.T.P., J.C.M., and N.M.H. designed research; E.T.P., N.T.W., I.H., E.A.E., C.B.E., and H.N.B. performed research; E.T.P., N.T.W., E.A.E., C.B.E., and N.M.H. analyzed data; I.H., E.A.E., and C.B.E. contributed new reagents/analytic tools; and E.T.P., J.C.M., A.J.T., and N.M.H. wrote the paper.

The authors declare no conflict of interest.

This article is a PNAS Direct Submission.

Abbreviations: Aβ, amyloid β; AD, Alzheimer's disease; APP, amyloid precursor protein; BACE1, β-site APP cleaving enzyme; CJD, Creutzfeldt–Jakob disease; GAG, glycosaminoglycan; GSS, Gerstmann–Scheinker–Straussler; LMW, low molecular weight; PrP, prion protein; PrP^C, cellular form of PrP; PrP^{Sc}, infectious form of PrP; sAPPα, soluble ectodomain of APP after α-cleavage; sAPPβ, soluble ectodomain of APP after β-cleavage; TSE, transmissible spongiform encephalopathy.

‡Present address: Department of Biological Sciences, Lancaster University, Lancaster LA1 4YQ, United Kingdom.

**To whom correspondence should be addressed. E-mail: n.m.hooper@leeds.ac.uk.

This article contains supporting information online at www.pnas.org/cgi/content/full/0609621104/DC1.

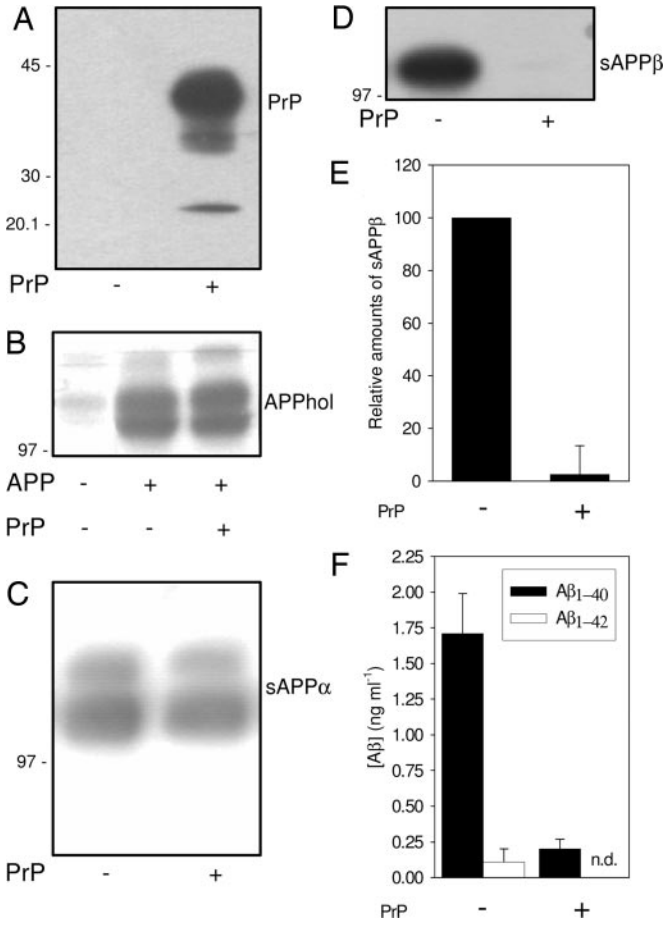

Fig. 1. PrP^C inhibits the β-secretase cleavage of APP. SH-SY5Y cells expressing APP_{695} were stably transfected with cDNA-encoding murine PrP. (*A*) Detection of PrP^C in cell lysates with 3F4. (*B*) Detection of the APP in cell lysates with Ab54. (*C*) Detection of sAPPα in conditioned medium with 6E10. (*D*) Detection of sAPPβ in conditioned medium with 1A9. (*E*) Quantification of multiple sAPPβ immunoblots by densitometric analysis. The amount of sAPPβ secreted from cells expressing PrP^C is expressed as a percentage of the amount secreted from mock transfected cells. (*F*) ELISA quantification of Aβ in conditioned medium. In all cases, the results are the mean ± SD of three independent experiments. n.d., not detected.

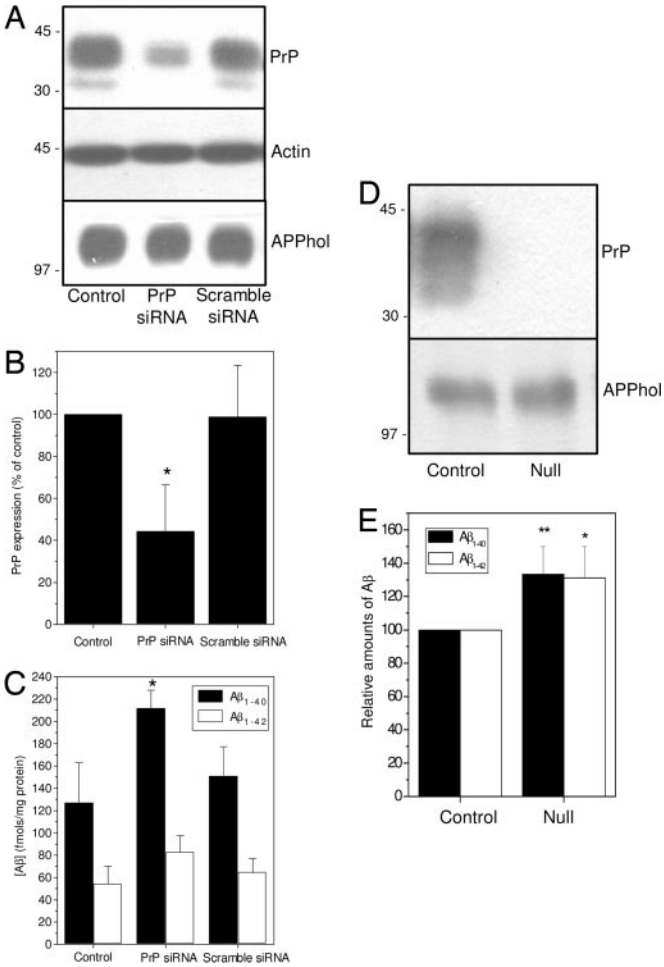

Fig. 2. Depletion of PrP^C increases Aβ peptide production. N2a cells were transfected with siRNA targeted against PrP or a scramble siRNA. (*A*) Detection in cell lysates of PrP with SAF-32, APP, and actin. (*B*) Quantification of multiple PrP immunoblots by densitometric analysis. (*C*) ELISA quantification of Aβ in conditioned medium. The results are the mean ± SD of four independent experiments. *, $P \leq 0.05$. Homogenates were prepared from control and PrP-null mouse forebrains. (*D*) Detection of PrP with SAF-32 and of APP with Ab54. (*E*) ELISA quantification of Aβ in mouse forebrain homogenates. The amount of Aβ is expressed as a percentage of the amount in control brain (means ± SD; $n = 4$ controls, $n = 9$ nulls). *, $P \leq 0.05$; **, $P \leq 0.005$.

of the β-secretase cleavage of APP, rather than an effect on γ-secretase. One possible explanation for this observation would be an alteration in the levels of expression of BACE1. However, the presence of PrP^C had no significant effect on the level of expression of BACE1 (SI Fig. 7). Another possibility is that PrP^C is competing with APP as a substrate for BACE1. However, neither the shedding nor the endoproteolytic processing of PrP^C was increased in cells overexpressing BACE1 (SI Fig. 8), indicating that PrP^C is not processed by BACE1.

Reduction of PrP by siRNA Increases Aβ Production, and Aβ Levels Are Increased in the Brains of PrP-Null Mice. To confirm that PrP^C regulates the production of Aβ in another cell system and using a different approach, we used siRNA duplexes to down-regulate the expression of endogenous PrP^C in the mouse neuroblastoma N2a cell line. The specific siRNA reduced the level of PrP^C expression by 60%, whereas the scrambled siRNA had no effect (Fig. 2 *A* and *B*). Cells treated with the specific siRNA had no difference in the amount of APP holoprotein (Fig. 2*A*). However, cells depleted of PrP^C secreted increased amounts of $A\beta_{1–40}$ and $A\beta_{1–42}$ into the conditioned medium compared to untreated cells or those treated with the scrambled siRNA (Fig. 2*C*).

To determine whether a reduced level of PrP^C would lead to increased Aβ levels in the brain, we compared the amount of Aβ in brains from $129OlaPrP^{-/-}$ mice to that in wild-type 129Ola controls. PrP was undetectable in the $PrP^{-/-}$ mice, whereas the level of APP holoprotein was similar to that in the wild-type mice (Fig. 2*D*). However, the levels of both $A\beta_{1–40}$ and $A\beta_{1–42}$ were significantly increased in the $PrP^{-/-}$ mice (Fig. 2*E*), providing direct evidence that PrP^C regulates the production of Aβ in the brain. It should be noted that increased levels of murine Aβ do not result in amyloid plaque deposition (16). A recent study reported that bigenic mice carrying mutant human APP and wild-type Syrian hamster PrP had increased amyloid plaques but no significant alteration in $A\beta_{1–40}$ or $A\beta_{1–42}$ levels compared to control mice carrying just the mutant APP (17). Because these control mice have endogenous levels of murine PrP^C, which may be maximally inhibiting the β-cleavage of APP (see Fig. 1), the overexpression of hamster PrP^C may not then lead to further inhibition of APP processing and Aβ production, but instead may have a secondary affect on Aβ aggregation.

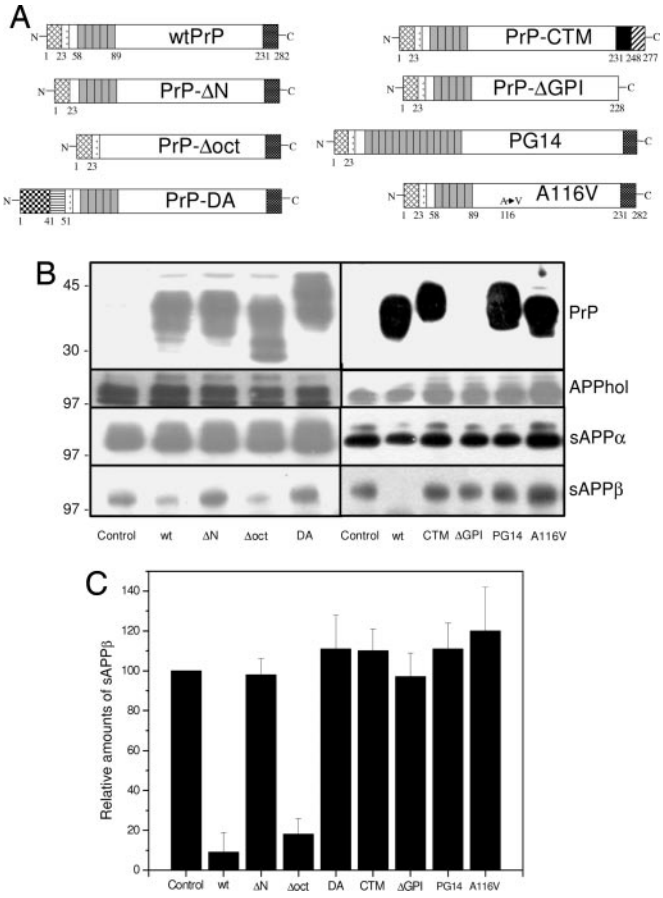

Fig. 3. The polybasic N terminus of PrP^C and its localization to lipid rafts are required for the inhibition of β-secretase. (*A*) Schematic of the PrP constructs used. Murine wtPrP comprises a 22-aa N-terminal sequence (criss-cross box), a positively charged N-terminal region (+++), a copper-binding octapeptide repeat region (gray shaded boxes), and a 23-aa C-terminal GPI anchor addition sequence (black box). PrPΔN lacks the four N-terminal residues (KKRP), and PrPΔoct lacks the octapeptide repeats (residues 51–90). PrP-DA retains the C-terminal GPI addition sequence, but the N-terminal signal peptide was replaced with the uncleaved signal sequence/transmembrane domain (checkered box) and stalk region (horizontal lined box) from murine aminopeptidase A. In PrP-CTM, the C-terminal GPI signal sequence was replaced with the transmembrane (black box) and cytosolic (hatched box) domains from angiotensin-converting enzyme. In PrPΔGPI, residues 229–254 of PrP, comprising the C-terminal GPI signal sequence, were deleted. PG14 contains an extra nine copies of the octapeptide repeat, and in A116V, Ala^{116} (murine PrP numbering, equivalent to Ala^{117} in human PrP) is mutated to Val. (*B*) SH-SY5Y cells expressing APP_{695} were stably transfected with the indicated PrP construct. Detection in cell lysates of PrP with 3F4 and of APP with Ab54. PrP-ΔGPI is not detected in the cell lysate because it lacks the membrane anchor and is secreted from the cell. Detection in the conditioned medium of sAPPα and sAPPβ. (*C*) Quantification of multiple sAPPβ immunoblots by densitometric analysis. The amount of sAPPβ secreted from cells expressing the PrP constructs is expressed as a percentage of the amount secreted from mock transfected cells. The results are the mean ± SD of three independent experiments.

The Polybasic N Terminus of PrP^C and Its Localization to Lipid Rafts Are Required for the Inhibition of β-Secretase. To determine the mechanism by which PrP^C inhibits the β-secretase cleavage of APP, we examined the effect of a number of PrP constructs (Fig. 3*A*). All of the anchored PrP constructs were expressed in the SH-SY5Y cells at a very similar level to wild-type PrP (Fig. 3*B*), and, as shown previously (18–20), all were present at the cell surface. The amount of APP_{695} holoprotein in the lysates from the cells expressing the different PrP constructs was similar, and no significant difference was detected in the shedding of sAPPα from any of the cell lines (Fig. 3*B*). However, although sAPPβ shedding, which is a direct measure of β-secretase activity, was dramatically reduced from cells transfected with either wild-type PrP or PrPΔoct, none of the other constructs had any significant effect on sAPPβ shedding (Fig. 3*C*), excluding the possibility that an overexpression artifact might cause the observed reduction in β-cleavage of APP. Because PrPΔoct inhibited the β-cleavage of APP similarly to wild-type PrP, the copper binding octapeptide repeats are not required for this effect. The lack of inhibitory effect on sAPPβ production by PrPΔN, which is missing the four residues (KKRP) at the N terminus of the mature protein, and PrP-DA, in which the N terminus is tethered to the membrane, indicate that the N-terminal polybasic region is critically required for PrP^C to inhibit the β-cleavage of APP. Neither PrPΔGPI, which is not membrane-attached, nor PrP-CTM, which is anchored by a transmembrane domain and is excluded from cholesterol-rich lipid rafts (19), reduced sAPPβ shedding. Thus, to inhibit the β-cleavage of APP, it would appear that PrP^C has to be localized to cholesterol-rich lipid rafts. This conclusion would be consistent with rafts being the site where the processing of APP by BACE1 preferentially occurs (21, 22), although there is a report that BACE1 can cleave APP outside of rafts (23).

The Inhibitory Action of PrP^C on β-Secretase Involves GAGs. Next we investigated whether PrP^C directly interacts with BACE1. Coimmunoprecipitation experiments demonstrated that PrP^C physically interacts with BACE1, but not with APP (Fig. 4*A*). However, PrP^C did not inhibit the activity of BACE1 toward a quenched fluorescent peptide substrate (SI Fig. 9), indicating that PrP^C does not regulate the processing of APP through direct inhibition of the enzymatic activity of BACE1. Because the N-terminal region of PrP, which is ablated in PrPΔN, is known to participate in GAG binding (24), we investigated whether GAGs are involved in the mechanism by which PrP^C inhibits the β-secretase cleavage of APP. Although wild-type PrP bound to heparin-coated ELISA plates in a concentration-dependent manner, PrPΔN did not bind above background levels (Fig. 4*B*), indicating that the N-terminal KKRP sequence is necessary for the binding of GAGs to PrP. We next investigated whether incubating cells with heparin could reverse the effect of PrP^C on the amyloidogenic processing of APP. Incubation of SH-SY5Y cells with heparin had no effect on the expression level of the APP holoprotein or on the shedding of sAPPα (Fig. 4*C*). In contrast, heparin increased the amount of sAPPβ shed from the cells in a concentration-dependent manner (Fig. 4 *C* and *D*) and reduced to 41.2 ± 7.3% ($n = 3$) the amount of BACE1 coimmunoprecipitated with PrP (Fig. 4*A*). Although heparin increased sAPPβ production in the absence of PrP^C, the fold increase in sAPPβ production was higher in the cells expressing PrP^C (2.16 ± 0.22-fold compared to 6.22 ± 1.22-fold, respectively) (Fig. 4*E*), thus showing that PrP^C is required to obtain the maximal effect of heparin on sAPPβ shedding.

Having established that heparin could restore sAPPβ shedding from cells expressing PrP and disrupt the physical interaction between PrP^C and BACE1 (Fig. 4 *A–E*), we investigated whether other GAGs could restore sAPPβ production and, if so, whether the same GAGs were also capable of binding to PrP^C. SH-SY5Y cells expressing wild-type PrP were incubated with hyaluronic acid, dextran sulfate, chondroitin sulfate A, low molecular weight (LMW) heparin, or polymerized heparin. None of the GAGs affected the level of APP holoprotein or the shedding of sAPPα, except for hyaluronic acid, which slightly reduced the amount of holoprotein and the shedding of sAPPα (Fig. 4*F*). In contrast, dextran sulfate and LMW heparin restored sAPPβ shedding to 55% and 47%, respectively, of that from untransfected cells, whereas heparin restored the level of sAPPβ shedding to 62% (Fig. 4 *F* and *G*). Hyaluronic acid and chondroitin sulfate A both failed to restore the shedding of sAPPβ (Fig. 4 *F* and *G*). We next examined the binding of the various GAGs to PrP^C (Fig. 4*H*). Relative to heparin,

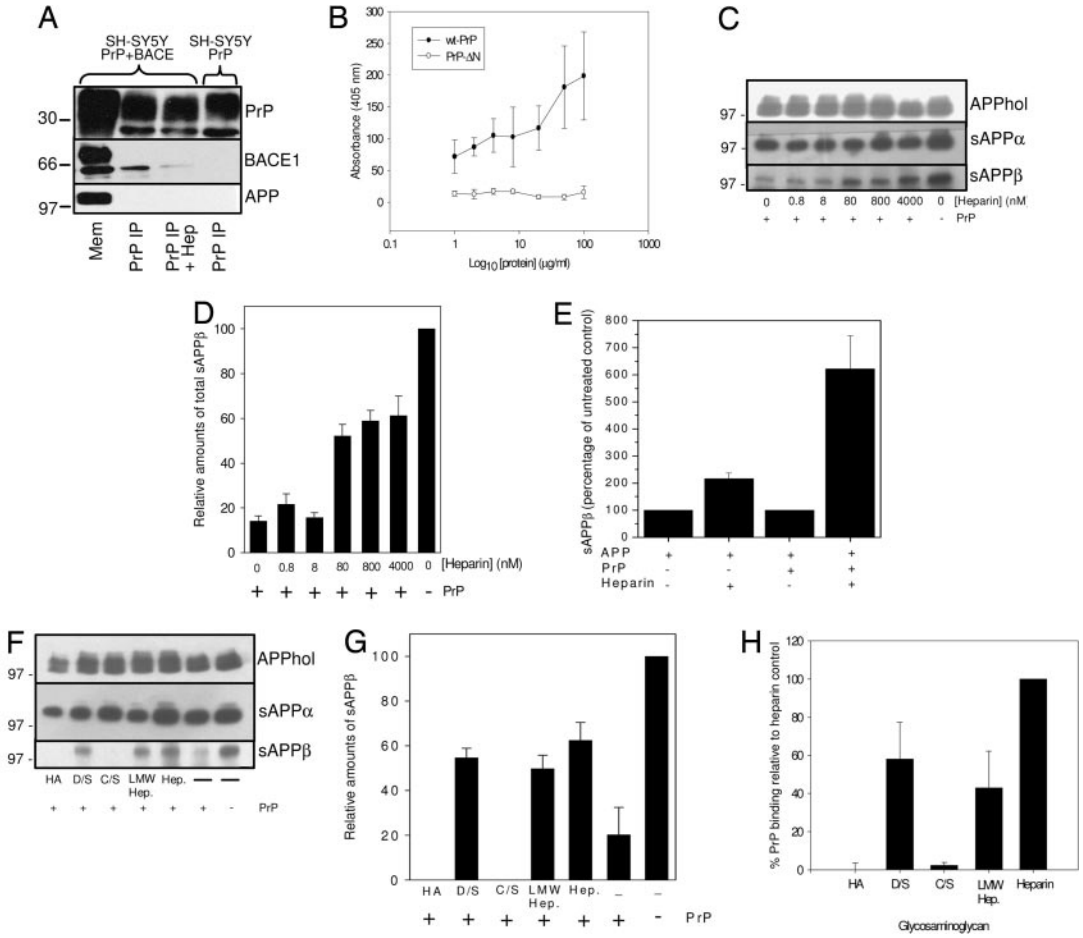

Fig. 4. The effect of GAGs on APP metabolism correlates with their binding to PrP^C. (*A*) Membranes from SH-SY5Y cells expressing PrP and BACE1 were solubilized with CHAPSO, immunoprecipitated with 3F4 in the absence or presence of 4 μM heparin, and the immunoprecipitates blotted for PrP, BACE1, and APP. Membranes were also prepared from cells expressing PrP, but not BACE1, and subjected to identical immunoprecipitation. (*B*) Increasing concentrations of lysate protein from cells expressing either wild-type PrP or PrPΔN were incubated in heparin precoated ELISA plate wells. The amount of bound PrP was determined by using 3F4 and secondary peroxidase-conjugated rabbit anti-mouse IgG, followed by the addition of ABTS and absorbance measurement at 405 nm. (*C*) SH-SY5Y cells expressing APP_{695} were stably transfected with the cDNA encoding wild-type PrP and incubated with the indicated concentration of heparin. Detection in cell lysates of APP and detection in conditioned medium of sAPPα and sAPPβ. (*D*) Quantification of multiple sAPPβ immunoblots by densitometric analysis. The amount of sAPPβ secreted from cells is expressed as a percentage of the amount secreted from untreated APP overexpressing cells. (*E*) SH-SY5Y cells expressing only APP_{695} and cells expressing both APP_{695} and wild-type PrP were incubated with 4 μM heparin. Conditioned medium was immunoblotted for sAPPβ, and multiple immunoblots were quantified by densitometric analysis. The amount of sAPPβ secreted from heparin-treated cells is expressed as a percentage of the amount secreted from the respective untreated control. (*F*) SH-SY5Y cells expressing APP_{695} were stably transfected with the cDNA encoding wild-type PrP and incubated with the indicated GAG. APP, sAPPα, and sAPPβ were detected as described in *C*. (*G*) Quantification of multiple sAPPβ immunoblots by densitometric analysis. The amount of sAPPβ secreted from cells is expressed as a percentage of the amount secreted from untreated APP overexpressing cells. (*H*) Cell lysate protein from wild-type PrP transfected cells was incubated in GAG precoated ELISA plate wells as in *B*. Results are expressed as the level of binding relative to heparin. HA, hyaluronic acid; D/S, dextran sulfate; C/S, chondroitin sulfate A; Hep, heparin; LMW Hep, low molecular weight hep. All results are the mean $\pm$ SD of three independent experiments, except for those results in *H*, which are the mean $\pm$ SEM of four independent experiments.

dextran sulfate and LMW heparin bound to wild-type PrP with 58% and 43% efficiencies, respectively. In contrast, hyaluronic acid and chondroitin sulfate A did not bind to wild-type PrP. Thus, those GAGs that were capable of binding to PrP^C were also able to restore the β-cleavage of APP, and the extent of binding to PrP^C directly correlated with the effect on APP processing. Because heparin has been shown to interact directly with BACE1 (25), a possible mechanism by which PrP^C regulates the β-cleavage of APP is through the N terminus of PrP^C interacting via GAGs with one or more of the heparin binding sites on BACE1 within a subset of cholesterol-rich lipid rafts, thereby restricting access of BACE1 to APP.

Aβ Levels Are Increased in Cells Expressing Disease-Associated Mutants of PrP and in Scrapie-Infected Brain. Two mutants of PrP, PG14 and A116V, which are associated with familial CJD and GSS, respectively (26, 27), did not inhibit the β-cleavage of APP when expressed in the SH-SY5Y cells (Fig. 3), suggesting that in certain forms of prion disease due to mutations in PrP there may be an increase in the production of Aβ. During prion disease, the proteinase-sensitive PrP^C undergoes a conformational conversion to the proteinase-resistant PrP^{Sc} and may lead to an alteration in the β-cleavage of APP. In the brains of two strains (79A and 87V) of scrapie-infected mice, there was a significant increase in the amount of proteinase K-resistant PrP^{Sc} (Fig. 5*A*). Although the level of APP holoprotein was unchanged between uninfected control mice and the scrapie-infected mice (Fig. 5*B*), the amount of Aβ was increased significantly in the scrapie-infected mice (Fig. 5*C*). Interestingly the amounts of $A\beta_{1-40}$ and $A\beta_{1-42}$ were higher in the mice with the shorter prion disease incubation time (79A, 146 days; 87V, 350 days). These results suggest that during prion disease, when PrP^C undergoes a conformational conversion to PrP^{Sc}, the inhibition of

NEUROSCIENCE

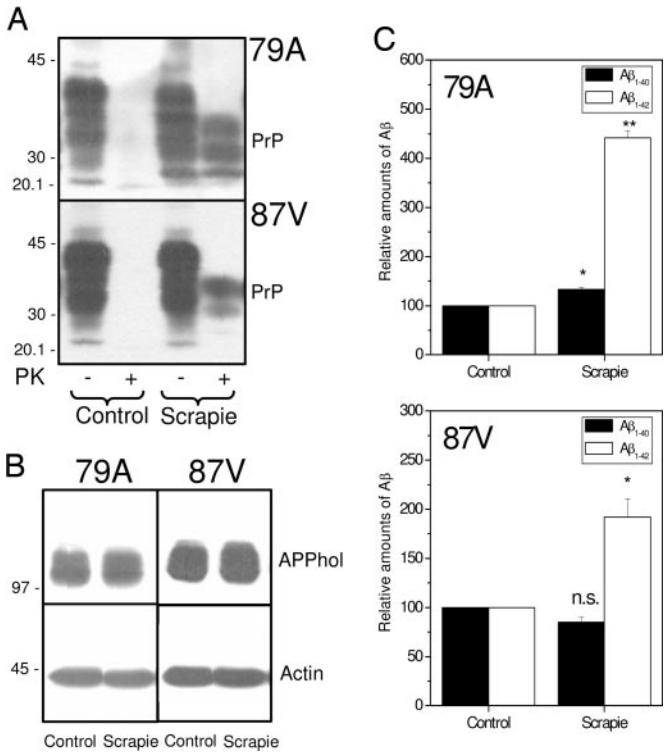

Fig. 5. Scrapie infection increases Aβ peptide production. Mice infected with scrapie strains 79A or 87V were killed at 146 and 350 days, respectively. The right cerebral hemisphere from each mouse was used to prepare soluble and membrane fractions, and the left hemisphere was used for Aβ extraction. (*A*) Detection of PrP^C and PrP^{Sc} in detergent-solubilized membrane fractions. Total membrane fractions were solubilized and incubated in the absence or presence of 20 μg/ml proteinase K for 1 h before immunoblotting with 6H4. (*B*) Detection in the membrane fraction of APP with 22C11 and actin. (*C*) ELISA quantification of Aβ in cerebral hemisphere homogenates. The amount of Aβ is expressed as a percentage of the amount in control brain (means $\pm$ SD, $n = 6$). *, $P \leq 0.05$; **, $P \leq 0.005$; n.s., not significant.

β-cleavage of APP may be lost, resulting in an increase in the amount of Aβ.

To investigate whether the Val/Met-129 polymorphism in human PrP^C would alter the production of Aβ, brains from mice whose endogenous *PrP* gene had been replaced with the human *PrP* gene with MM or VV 129 genotypes (28) were analyzed. Although there was no difference in the amount of $A\beta_{1-42}$ (0.188 $\pm$ 0.015 vs. 0.184 $\pm$ 0.015 pmol/g; $P = 0.348$) between the MM and VV homozygous mice, respectively, there was a significant increase in the amount of $A\beta_{1-40}$ (0.359 $\pm$ 0.026 vs. 0.324 $\pm$ 0.015 pmol/g; $P = 0.014$) in the MM mice compared to the VV mice.

Conclusions

We have identified a new role for PrP^C in inhibiting the β-secretase cleavage of APP, thereby regulating the production of the neurotoxic Aβ peptide. Our data would predict that the lack of functional PrP^C would lead to an increase in Aβ levels and potentially AD in humans. In this respect, in the two cases where a mutation ($Y145^{stop}$ or $Q160^{stop}$) gives rise to truncated forms of PrP that fail to traffic to the cell surface, a diagnosis of AD was made, with the onset of clinical disease occurring in the fourth decade of life (29, 30). It is conceivable that small changes in PrP^C levels in individuals may affect the proteolytic processing of APP in a subtle way over decades to affect long-term Aβ production that, in turn, could either accelerate or decelerate the deposition of amyloid in the brain. Our observations that the level of Aβ increases in scrapie-infected mice brains when PrP^C is converted to PrP^{Sc} and that mutations in PrP that give rise to human prion diseases ablate the inhibitory effect of PrP^C on the β-cleavage of APP suggest that the inhibition of β-secretase by PrP^C is released in both TSEs and inherited prion diseases. Whether the increase in Aβ is, in part, responsible for the neurodegeneration observed in prion diseases and whether the increase in Aβ seen in humanized MM mice is linked to the Met/Val-129 polymorphism being a risk factor for early onset AD (11) awaits further study. In addition, these observations raise significant questions over whether depletion of PrP^C (31) is a sound therapeutic approach for TSEs, but suggest that pharmacological interventions that mimic the effect of PrP^C in inhibiting the β-secretase cleavage of APP may represent a therapeutic approach for AD.

Materials and Methods

Cell Culture and Plasmids. The SH-SY5Y cell line was cultured and cell lysates and conditioned medium were collected as described previously (32). Insertion of the coding sequence of murine PrP containing a 3F4 epitope tag into pIRESneo (BD Biosciences Clontech, Palo Alto, CA) and the generation of the PrP constructs have been reported previously (18, 20, 32). The coding sequence of human APP_{695} was inserted into the BstX I site of pIREShyg (BD Biosciences Clontech). The coding sequence of human BACE1 was inserted into the BamH I and BstX I sites of pIREShyg. For stable transfections, 30 μg of DNA was introduced to cells by electroporation and selection was performed in normal growth medium containing 500 μg/ml neomycin or 100 μg/ml hygromycin B (Gibco BRL, Paisley, U.K.). The cells were preincubated for 24 h in OptiMEM containing the stated GAG concentrations, washed *in situ* with OptiMEM, and incubated for a further 7 h in fresh OptiMEM containing the GAGs.

siRNA Transfection. siRNAs corresponding to the murine *Prnp* gene from codon 392 to 410 (33) were synthesized by Dharmacon RNA Technologies (Lafayette, CO) and were supplied preduplexed. The sequences of the siRNAs are detailed in *SI Methods*. N2a cells were seeded at 10–15% confluency in a 12-well plate 24 h before transfection. siRNA (10 μl of the stock solution) was mixed with the corresponding half-volume of Oligofectamine reagent (Invitrogen, Paisley, U.K.) for 20 min and applied to the cells in a final volume made up to 0.5 ml with Opti-MEM. After incubation for 4 h at 37°C, 0.25 ml of Opti-MEM supplemented with 30% FBS and a penicillin/streptomycin mixture was added. Cells were cultured for 3 days at 37°C until confluent, after which medium was conditioned for 24 h.

Animals. Inbred PrP knockout mice ($129OlaPrP^{-/-}$) and 129Ola wild-type mice (34), and mice whose endogenous PrP gene had been replaced with the human PrP gene with MM or VV 129 genotypes (28), were analyzed at 4 weeks of age. Mice infected with scrapie strains 79A and 87V along with their respective age-matched controls were killed by cervical dislocation at 146 and 350 days, respectively, and the brains were immediately removed, rinsed in PBS, frozen in liquid nitrogen, and stored at −80°C before Aβ analysis. Animal care was in accordance with institutional guidelines.

Mouse Forebrain Fractionation and Proteinase K Treatment. Cerebral hemispheres from killed mice were homogenized in 10 volumes of buffer A [5 mM Tris·HCl, 250 mM sucrose, 1 mM EGTA, and 5 mM EDTA (pH 7.4) containing a protease inhibitor mixture] by using 30 passes of a Dounce homogenizer. The homogenates were centrifuged at 5,000 $\times$ *g* for 10 min, and the resultant supernatant was centrifuged at 100,000 $\times$ *g* for 1 h. The supernatant (soluble fraction) was removed and the membrane pellet resuspended in 200 μl of buffer A lacking sucrose. For proteinase K digestion, aliquots of the resuspended membrane pellet were detergent-solubilized by

the addition of an equal volume of buffer A lacking sucrose but containing 1% (wt/vol) sodium deoxycholate and 1% (vol/vol) Nonidet P-40. The samples were incubated at 4°C for 1 h and then centrifuged for 10 min at 11,600 × *g*. The detergent-soluble supernatant was incubated in the absence or presence of 20 μg/ml proteinase K for 1 h at 37°C.

Immunoprecipitation, SDS/PAGE, and Immunoelectrophoretic Blot Analysis. Proteins were immunoprecipitated and resolved by SDS/PAGE by using 7–17% polyacrylamide gradient gels and transferred to Immobilon P poly(vinylidene difluoride) membranes as previously described (32, 35). Antibody 3F4 recognizes an epitope tag at residues 108–111 of the murine prion protein, and antibody 6E10 recognizes amino acid residues 1–17 of the human Aβ sequence (both Signet Laboratories, Dedham, MA). Antibody 6H4 (Prionics AG, Zurich, Switzerland) recognizes the sequence DYEDRYYRE (human PrP: amino acids 144–152). Ab54 recognizes the C-terminal region of APP, and antibody 1A9 recognizes a neoepitope on sAPPβ formed after β-secretase cleavage of APP (36). Antibody 9B21 was raised to the catalytic domain of BACE1 by using BACE1-Fc fusion protein as immunogen. Antibody 22C11 (Chemicon International, Temecula, CA) recognizes amino acid residues 66–81 in the N terminus of APP. Antibody SAF-32 (Cayman Chemical, Ann Arbor, MI) recognizes the octapeptide repeat region located in the N-terminal region of PrP. Bound antibody was detected by using peroxidase-conjugated secondary antibodies in conjunction with the enhanced-chemiluminescence (ECL) detection method (Amersham Life Sciences, Buckinghamshire, U.K.).

ELISA Quantification of Aβ Peptides. Mouse forebrains were homogenized in 10 volumes of 0.2% (vol/vol) diethylamine in 50 mM NaCl by 35 passes of a Dounce homogenizer. The homogenate was then centrifuged at 100,000 × *g* for 1 h, and the supernatants were neutralized by the addition of 1/10 volume of 0.5 M Tris·HCl (pH 6.8). The brain homogenates or conditioned medium from N2a cells (100 μl) was added to assay plates containing 50 μl of 0.02 M sodium phosphate (pH 7.0), 2 mM EDTA, 0.4 M NaCl, 0.2% BSA, 0.05% CHAPS, 0.4% Block Ace, 0.05% NaN_3 and analyzed by using the BNT77/BA27 and BNT77/BC05 sandwich ELISA systems to detect $A\beta_{1-40}$ and $A\beta_{1-42}$, respectively (37). Human $A\beta_{1-40}$ and $A\beta_{1-42}$ in conditioned medium from SH-SY5Y cells were captured by using biotinylated 6E10. BioVeris-tagged Aβ C-terminal specific antibodies were then used to detect $A\beta_{1-40}$ and $A\beta_{1-42}$. Antibody–Aβ complexes were captured with streptavidin-coated dynabeads and assayed in a BioVeris M8 analyzer. Standard curves were constructed by using $A\beta_{1-40}$ and $A\beta_{1-42}$ dissolved in DMSO.

ELISA Quantification of GAG Binding to PrP^C. ELISAs were performed as described previously (38). Plates were coated with the desired GAG before blocking the wells with 3% BSA in PBS. After washing with PBS-Tween (0.05%), cell lysate protein was added over a concentration range of 1 to 100 μg/ml. After a 2-h incubation at room temperature, the plate was washed three times with PBS-Tween (0.05%) and incubated with a 1:3,000 dilution of 3F4 overnight at 4°C. The plate was washed three times with PBS-Tween (0.05%), and peroxidase-conjugated rabbit anti-mouse IgG was added to the wells. After a 1-h incubation at room temperature, the plate was washed by using PBS-Tween (0.05%) and 2,2′-azinobis-(3-ethylbenzothiazoline-6-sulfonic acid) (Roche Diagnostics Ltd., East Sussex, U.K.), and the absorbance was measured at 405 nm.

Statistical Analyses. Results are given as mean ± SD. Statistical analyses were performed by using Student's *t* test (two-tailed), and the null hypothesis was rejected at the 0.05 level.

We thank Takeda Chemical Industries for the BNT77, BA27, and BC05 antibodies. This work was supported by Medical Research Council of Great Britain Grant G9824728 (to A.J.T. and N.M.H.), European Union Grant QLG3-CT-2001–02353 (to N.M.H.), National Institutes of Health Grants NS042192 and NS048554–01 (to C.B.E.), the Alzheimer's Association (E.A.E.), the Robert H. and Clarice Smith and Abigail Van Buren Alzheimer's Disease Research Program, and the Mayo Foundation for Medical Education and Research (C.B.E. and E.A.E.). A.J.T. and N.M.H. are members of the Yorkshire Centre in the Alzheimer's Research Trust's Alzheimer's Disease Research Centre Network.

1. Selkoe DJ (2001) *Physiol Rev* 81:741–766.
2. Haass C (2004) *EMBO J* 23:483–488.
3. Allinson TM, Parkin ET, Turner AJ, Hooper NM (2003) *J Neurosci Res* 74:342–352.
4. Aguzzi A, Montrasio F, Kaeser PS (2001) *Nat Rev Mol Cell Biol* 2:118–126.
5. Brown DR (2001) *Trends Neurosci* 24:85–90.
6. Martins VR, Linden R, Prado MA, Walz R, Sakamoto AC, Izquierdo I, Brentani RR (2002) *FEBS Lett* 512:25–28.
7. Powers JM, Liu Y, Hair LS, Kascsack RJ, Lewis LD, Levy LA (1991) *Acta Neuropathol (Berl)* 83:95–98.
8. Hainfellner JA, Wanschitz J, Jellinger K, Liberski PP, Gullotta F, Budka H (1998) *Acta Neuropathol (Berl)* 96:116–122.
9. Voigtlander T, Kloppel S, Birner P, Jarius C, Flicker H, Verghese-Nikolakaki S, Sklaviadis T, Guentchev M, Budka H (2001) *Acta Neuropathol (Berl)* 101:417–423.
10. Dermaut B, Croes EA, Rademakers R, Van den Broeck M, Cruts M, Hofman A, van Duijn CM, Van Broeckhoven C (2003) *Ann Neurol* 53:409–412.
11. Riemenschneider M, Klopp N, Xiang W, Wagenpfeil S, Vollmert C, Muller U, Forstl H, Illig T, Kretzschmar H, Kurz A (2004) *Neurology* 63:364–366.
12. Buxbaum JD, Liu K-N, Luo Y, Slack JL, Stocking KL, Peschon JJ, Johnson RS, Castner BJ, Cerretti DP, Black RA (1998) *J Biol Chem* 273:27765–27767.
13. Allinson TM, Parkin ET, Condon TP, Schwager SL, Sturrock ED, Turner AJ, Hooper NM (2004) *Eur J Biochem* 271:2539–2547.
14. Vincent B, Paitel E, Saftig P, Frobert Y, Hartmann D, De Strooper B, Grassi J, Lopez-Perez E, Checler F (2001) *J Biol Chem* 276:37743–37746.
15. Parkin ET, Watt NT, Turner AJ, Hooper NM (2004) *J Biol Chem* 279:11170–11178.
16. Andersen OM, Reiche J, Schmidt V, Gotthardt M, Spoelgen R, Behlke J, von Arnim CAF, Breiderhoff T, Jansen P, Wu X, *et al*. (2005) *Proc Natl Acad Sci USA* 102:13461–13466.
17. Schwarze-Eicker K, Keyvani K, Gortz N, Westaway D, Sachser N, Paulus W (2005) *Neurobiol Aging* 26:1177–1182.
18. Perera WSS, Hooper NM (2001) *Curr Biol* 11:519–523.
19. Taylor DR, Watt NT, Perera WS, Hooper NM (2005) *J Cell Sci* 118:5141–5153.
20. Watt NT, Taylor DR, Gillott A, Thomas DA, Perera WS, Hooper NM (2005) *J Biol Chem* 280:35914–35921.
21. Cordy JM, Hussain I, Dingwall C, Hooper NM, Turner AJ (2003) *Proc Natl Acad Sci USA* 100:11735–11740.
22. Ehehalt R, Keller P, Haass C, Thiele C, Simons K (2003) *J Cell Biol* 160:113–123.
23. Abad-Rodriguez J, Ledesma MD, Craessaerts K, Perga S, Medina M, Delacourte A, Dingwall C, De Strooper B, Dotti CG (2004) *J Cell Biol* 167:953–960.
24. Warner RG, Hundt C, Weiss S, Turnbull JE (2002) *J Biol Chem* 277:18421–18430.
25. Scholefield Z, Yates EA, Wayne G, Amour A, McDowell W, Turnbull JE (2003) *J Cell Biol* 163:97–107.
26. Krasemann S, Zerr I, Weber T, Poser S, Kretzschmar H, Hunsmann G, Bodemer W (1995) *Brain Res Mol Brain Res* 34:173–176.
27. Hegde RS, Mastrianni JA, Scott MR, DeFea KA, Tremblay P, Torchia M, DeArmond SJ, Prusiner SB, Lingappa VR (1998) *Science* 279:827–834.
28. Bishop MT, Hart P, Aitchison L, Baybutt HN, Plinston C, Thomson V, Tuzi NL, Head MW, Ironside JW, Will RG, Manson JC (2006) *Lancet Neurol* 5:393–398.
29. Kitamoto T, Iizuka R, Tateishi J (1993) *Biochem Biophys Res Commun* 192:525–531.
30. Finckh U, Muller-Thomsen T, Mann U, Eggers C, Marksteiner J, Meins W, Binetti G, Alberici A, Hock C, Nitsch RM, Gal A (2000) *Am J Hum Genet* 66:110–117.
31. White AR, Enever P, Tayebi M, Mushens R, Linehan J, Brandner S, Anstee D, Collinge J, Hawke S (2003) *Nature* 422:80–83.
32. Walmsley AR, Zeng F, Hooper NM (2001) *EMBO J* 20:703–712.
33. Daude N, Marella M, Chabry J (2003) *J Cell Sci* 116:2775–2779.
34. Manson JC, Clarke AR, Hooper ML, Aitchison L, McConnell I, Hope J (1994) *Mol Neurobiol* 8:121–127.
35. Gu Y, Sanjo N, Chen F, Hasegawa H, Petit A, Ruan X, Li W, Shier C, Kawarai T, Schmitt-Ulms G, *et al*. (2004) *J Biol Chem* 279:31329–31336.
36. Parvathy S, Hussain I, Karran EH, Turner AJ, Hooper NM (1998) *Biochemistry* 37:1680–1685.
37. Scheuner D, Eckman C, Jensen M, Song X, Citron M, Suzuki N, Bird TD, Hardy J, Hutton M, Kukull W, *et al*. (1996) *Nat Med* 2:864–870.
38. Pan T, Wong BS, Liu T, Li R, Petersen RB, Sy MS (2002) *Biochem J* 368:81–90.